NATIONAL ADVISORY COMMITTEE FOR AERONAUTICS

TECHNICAL NOTE 1950

DAMPING-IN-ROLL CALCULATIONS FOR SLENDER SWEPT-BACK WINGS AND SLENDER WING-BODY COMBINATIONS

By Harvard Lomax and Max. A. Heaslet

Ames Aeronautical Laboratory
Moffett Field, Calif.

Washington
September 1949

NATIONAL ADVISORY COMMITTEE FOR AERONAUTICS

TECHNICAL NOTE 1950

DAMPING-IN-ROLL CALCULATIONS FOR SLENDER SWEPT-BACK WINGS AND SLENDER WING-BODY COMBINATIONS

By Harvard Lomax and Max. A. Heaslet

SUMMARY

The damping-in-roll parameter Cl_p is calculated theoretically for triangular wings on cylindrical bodies and for a class of wings with swept-back plan forms. The analysis is based on the usual assumptions of linearized compressible-flow theory together with the added restrictions that at the free-stream Mach number M_o the product of $1-M_o^2$ and the streamwise velocity gradient is small. The accuracy of the results is tested by a comparison with the exact solution of the linearized equation for a triangular wing and for such plan forms is shown to increase as reduced aspect ratio ($\sqrt{|1-M_o^2|}$ times aspect ratio) decreases.

INTRODUCTION

Theoretical advancements in the study of load distributions over three-dimensional wings in compressible-flow fields have been achieved almost entirely under assumptions leading to the linearization of the basic differential equations of flow. In this manner the analysis is resolved in general into the problem of determining solutions of elliptic and hyperbolic partial differential equations in three dimensions, the character of the equations being fixed by the magnitude of the free-stream Mach number M_o. It is possible, however, to study also a class of problems associated with the parabolic form of the potential equation; namely, cases for which the product of $1-M_o^2$ and the chordwise perturbation-velocity gradient is small in comparison with the gradients in their respective directions of the perturbation velocities perpendicular to the chord. Such a method was developed in reference 1 for small values of aspect ratio and was used in reference 2 for swept-back lifting surfaces at sonic speeds. In the present report the method will be referred to as a slender-wing theory wherein the term slender infers that the ratio of the reduced[1] span to the over-all length is small. Hence the results

[1]Reduced span is defined as β times the span, where β is equal to $\sqrt{|1-M_o^2|}$. In general, the term reduced implies that any parameter which it modifies is multiplied by the factor β.

presented will apply most closely when the wing is long in terms of its span, or when the free-stream Mach number is close to unity and the wing and body do not violate the assumptions made.

Previous investigations (references 3, 4, 5, and 6) corresponding to this method of approach include, respectively, a complete analysis of all the stability derivatives of a low-aspect-ratio triangular wing, a lifting triangular wing with an arbitrary body of revolution, a lifting triangular cruciform combination on an arbitrary body of revolution, and a lifting swept-back constant-chord wing. In order to assess the accuracy of the results presented in these reports, it is necessary to compare their approximate solutions with the exact solutions of the linearized equation. For the case of the rolling triangular wing, this can easily be done since the exact solution has been derived in reference 7. The results of such a comparison are presented in figure 1 which indicates that in this case the value of βC_{l_p} for the approximate theory can be useful up to reduced aspect ratios as high as three.

The object of the present report is three-fold: First, to find the effect on the damping-in-roll parameter C_{l_p} of adding a body of revolution to a triangular wing in order to extend the knowledge of wing-body interference into the field of lateral stability; second, to find C_{l_p} for a particular swept-back wing plan form; and third, to show how the damping due to roll can be found for swept wings with arbitrary trailing edges or how trailing edges can be calculated from prescribed span load distributions. The examples to be given provide sufficient details to indicate how other cases can be calculated numerically.

A list of important symbols is given in Appendix A.

RÉSUMÉ OF THE METHOD

Under the assumption that $(1-M_o^2)\Phi_{XX}$ is small as compared to Φ_{YY} and Φ_{ZZ}, the equation for compressible fluid motion, either subsonic or supersonic, becomes

$$\Phi_{YY} + \Phi_{ZZ} = 0 \qquad (1a)$$

where Φ is the perturbation-velocity potential and X is the free-stream flow direction. The resulting differential equation (1a) shows that although Φ can be a function of X its value is a consequence of boundary conditions given along lateral strips. We will seek solutions to equation (1a) for which first, the perturbation velocities vanish at infinity; second, there is no discontinuity in potential except across a lifting surface or its trailing vortex sheet; and third, there is no discontinuity in the vertical velocity anywhere in the field (i.e., no airfoil with thickness). It is possible, by applying the two-dimensional form of Green's theorem, to write the solution to equation (1a) which

satisfies all of the aforementioned conditions and relates w_{t_o} (Φ_Z in the Z = 0 plane) to Δv_{t_o} (the jump in sidewash, Φ_Y in the Z = 0 plane). Under the added restriction that no point exists in or on the flow field such that $\lim_{\epsilon \to 0} \epsilon \frac{\partial \Phi}{\partial \epsilon} \neq 0$, where ϵ is the radial distance from the point, this solution can be written[2]

$$w_{t_o} = -\frac{1}{2\pi} \int_{-B(X)}^{B(X)} \frac{\Delta v_{t_o} dY_1}{Y - Y_1} \tag{2a}$$

The integral equation (2a) will be solved for the case of rolling wings. First, however, it is convenient to introduce nondimensional lengths so that the results can be generalized as far as possible. A satisfactory nondimensional form is obtained by using the equations

$$\left.\begin{aligned} y &= \frac{Y}{C \tan \theta} & u &= C\, u_t \\ & & v &= C\, v_t \tan \theta \\ x &= \frac{X}{C} & w &= C\, w_t \tan \theta \\ & & v_r &= C\, v_{r_t} \tan \theta \\ z &= \frac{Z}{C \tan \theta} & \mu &= p\, C^2 \tan^2 \theta \end{aligned}\right\} \tag{3}$$

where θ is the semivertex angle of the wing, p is the rate of roll in radians per second, C is the root chord, u_t, v_t, w_t, and v_{r_t} are true of velocity components, and u, v, w, and v_r are the transformed components. In addition $\varphi(x,y,z)$ replaces $\Phi(X,Y,Z)$.

TRIANGULAR WING WITH BODY

Consider a wing with an unswept trailing edge mounted on a body of revolution as shown in figure 2. Applying the transformations given by equations (3) to equation (1a), we find that in every plane perpendicular to the x axis it is necessary to satisfy the equation

$$\varphi_{yy} + \varphi_{zz} = 0 \tag{1b}$$

[2]This equation is developed in more detail in reference 2.

subject to the boundary conditions

$$\left.\begin{aligned} v_r &= 0 \qquad \text{for} \quad r = a, \ 0 \le \psi \le 2\pi \\ w_o &= \mu y \qquad \text{for} \quad z = 0, \ a \le |y| \le b \\ w &= v = 0 \qquad \text{for} \quad r = \infty, \ 0 \le \psi \le 2\pi \end{aligned}\right\} \tag{4}$$

where $a(x)$ and $b(x)$ are replaced by a and b for convenience in notation and where r, ψ are polar coordinates in the yz plane and μ is related to the rate of roll by equation (3). These boundary conditions are not of a type such that they can be substituted directly into equation (2a), since one condition specifies a radial component which is, moreover, out of the $z = 0$ plane. However, equation (1) is simply Laplace's equation so that by introducing complex variables it is not difficult to transform the wing and body section (fig. 3(a)) to a strip along the y axis (fig. 3(b)). Such a mapping function is provided by the Joukowski transformation,[3] which, if the subscript 1 denotes conditions in the transformed plane, can be written:

$$\xi_1 = \xi + \frac{a^2}{\xi} \tag{5}$$

where ξ and ξ_1 are given by the expressions

$$\left.\begin{aligned} \xi &= y + iz \\ \xi_1 &= y_1 + iz_1 \end{aligned}\right\} \tag{6}$$

By means of equation (5) the wing in the ξ plane (the portion of the axis for which $a \le |y| \le b$, fig. 3) transforms into the section of the y_1 axis in the ξ_1 plane for which $2a = a_1 \le |y_1| \le b_1 = b + \frac{a^2}{b}$. Further, the body in the ξ plane (the curve satisfying the equation r=a) transforms into the part of the y_1 axis for which $0 \le |y_1| \le a_1 = 2a$. In this manner the boundary on which the data are specified has been transformed so that it lies entirely along the y_1 axis. It is next necessary to inspect what the boundary conditions are in the ξ_1 plane.

From the basic theory underlying the use of complex variables, induced velocities in the physical and transformed planes are related by the expression

$$v - iw = (v_1 - iw_1)\frac{d\xi_1}{d\xi} \tag{7}$$

[3]See, for example, "The Elements of Aerofoil and Airscrew Theory," Cambridge University Press, 1943, by H. Glauert.

from which, since in polar coordinates

$$\frac{d\xi_1}{d\xi} = \left[1 - \left(\frac{a}{r}\right)^2 \cos 2\psi\right] + i \left(\frac{a}{r}\right)^2 \sin 2\psi \tag{8}$$

it follows immediately that

$$\left.\begin{aligned} v &= v_1\left[1 - \left(\frac{a}{r}\right)^2 \cos 2\psi\right] + w_1 \left(\frac{a}{r}\right)^2 \sin 2\psi \\ w &= w_1\left[1 - \left(\frac{a}{r}\right)^2 \cos 2\psi\right] - v_1 \left(\frac{a}{r}\right)^2 \sin 2\psi \\ v_r &= \left[v_1 \cos\psi + w_1 \sin\psi\right]\left[1 - \left(\frac{a}{r}\right)^2\right] + 2 w_1 \left(\frac{a}{r}\right)^2 \sin\psi \end{aligned}\right\} \tag{9}$$

Through the use of equation (9), the boundary conditions given by equation (4) for the ξ plane can be transformed to the ξ_1 plane with the result (since $\psi = 0$ or π)

$$\left.\begin{aligned} &w_1 = 0 \quad \text{for} \quad 0 \le |y_1| \le a_1 \\ &w_1 = \frac{\mu}{4} \frac{y_1}{|y_1|} \frac{2y_1^2 - a_1^2}{\sqrt{y_1^2 - a_1^2}} + \frac{\mu}{2} y_1 \quad \text{for} \quad a_1 \le |y_1| \le b_1 \\ &v_1 = w_1 = 0 \quad \text{for} \quad r_1 = \infty, 0 \le \psi \le 2\pi \end{aligned}\right\} \tag{10}$$

The problem has now become one of solving Laplace's equation for the boundary conditions given by equation (10). But this problem can be immediately solved, provided we can invert the integral equation (2a), which in the new notation,[4] becomes

$$w_1(y_1) = -\frac{1}{2\pi} \int_{-b_1}^{b_1} \frac{\Delta v_1(y_2)\,dy_2}{y_1 - y_2} \tag{2b}$$

[4] Note that the subscript o (indicating conditions in the $Z_1 = 0$ plane) has been dropped when in the ξ_1 plane. This avoids a cumbersome notation and should cause no confusion, since in the ξ_1 plane only conditions on the y_1 axis are to be considered.

Under the condition

$$\int_{-b_1}^{b_1} \frac{w_1(y_1)dy_1}{\sqrt{b_1^2-y_1^2}} = 0 \tag{11}$$

reference 8 gives an inversion to equation (2b) which can be written

$$\Delta v_1(y_1) = \frac{2}{\pi}\sqrt{b_1^2-y_1^2}\int_{-b_1}^{b_1} \frac{w_1(y_2)dy_2}{(y_1-y_2)\sqrt{b_1^2-y_2^2}} + \frac{c_o}{\sqrt{b_1^2-y_1^2}} \tag{12}$$

where c_o is an arbitrary constant.

An inspection of w_1 as given by the boundary conditions in equation (10) shows that it is an odd function of y_1 and hence will satisfy equation (11). Placing w_1 in equation (12) and integrating gives

$$\Delta v_1(y_1) = -\frac{\mu(2y_1^2-a_1^2)}{2\sqrt{a_1^2-y_1^2}}\left(\frac{1-\sigma}{2}\right) - \frac{2\mu}{\pi}\sqrt{b_1^2-y_1^2}\left(\frac{\pi}{2} + \arccos\frac{a_1}{b_1}\right) -$$

$$\frac{\mu y_1}{\pi}\ln\left|\frac{y_1\sqrt{b_1^2-a_1^2} + a_1\sqrt{b_1^2-y_1^2}}{y_1\sqrt{b_1^2-a_1^2} - a_1\sqrt{b_1^2-y_1^2}}\right| + \frac{c_o}{\sqrt{b_1^2-y_1^2}} \tag{13}$$

where $\sigma = -1$ for $0 \leq |y_1| \leq a_1$, and $\sigma = +1$ for $a_1 \leq |y_1| \leq b_1$.

Now to find $\Delta\varphi_1$ on the $z_1 = 0$ plane, the relation

$$\Delta\varphi_1 = \int_{-b_1}^{y_1} \Delta v_1(y_2)dy_2 \tag{14}$$

in which $\Delta v_1(y_2)$ as given by equation (13) is used with the result that, for $a_1 \leq y_1 \leq b_1$,

$$\Delta\varphi_1 = -\frac{\mu}{2}\left(1 + \frac{2}{\pi}\arccos\frac{a_1}{b_1}\right)y_1\sqrt{b_1^2-y_1^2} -$$

$$\frac{\mu}{2\pi}(y_1^2-a_1^2)\operatorname{arc\,cosh}\frac{y_1\sqrt{b_1^2-a_1^2}}{b_1\sqrt{y_1^2-a_1^2}} \tag{15}$$

where the constant c_o has been evaluated by the conditions that $\Delta\varphi_1$ must vanish when $y_1 = b_1$. This can be written in terms of the original coordinates (fig. 2(b)) and boundary conditions (equation (4)), by retransforming in accordance with equation (5). Thus, for $a \leq y \leq b$,

$$\Delta\varphi_o = -\frac{\mu}{2}\left(1 - \frac{2}{\pi}\arccos\frac{2ab}{b^2 + a^2}\right)\left(y + \frac{a^2}{y}\right)\sqrt{b^2 + \frac{a^4}{b^2} - y^2 - \frac{a^4}{y^2}} - \frac{\mu}{2\pi}\left(y - \frac{a^2}{y}\right)\operatorname{arc\,cosh}\frac{(y^2+a^2)(b^2-a^2)}{(y^2-a^2)(b^2+a^2)} \tag{16}$$

Equation (16) represents the solution, in terms of the velocity potential, for a rolling wing with an unswept trailing edge on a body of revolution; both a and b are functions of x. The loading coefficient $\frac{\Delta p}{q}$ can be determined by taking the partial derivative of equation (16) with respect to x in order to find Δu, and then using the relation

$$\frac{\Delta p}{q} = \frac{2\Delta u_t}{V_o} = \frac{2\Delta u}{CV_o} \tag{17}$$

However, it is not necessary to find the loading over the wing if interest is limited to the determination of the total rolling moment L. If a is independent of x (i.e., the body is a circular cylinder), then $\Gamma = (\Delta\varphi)_{T.E.}$ and the equation

$$dl = \rho V_o \Gamma \, dY$$

where dl is the increment in span loading, can be used to express

$$dL = Y dl = \rho V_o Y \Gamma \, dY$$

Thus

$$L = 2\rho V_o \int_A^S Y(\Delta\Phi_o)_{T.E.} \, dY$$

or

$$L = 2\rho V_o C^2 \tan^2\theta \int_a^s y(\Delta\varphi_o)_{T.E.} \, dy \tag{18}$$

where $(\Delta\varphi_o)_{T.E.}$ is the value of $\Delta\varphi_o$ at the trailing edge or where $x = 1$ in figure 2(b). Substituting equation (16) in equation (18), one can derive, after some rather involved integration, the result

$$\frac{L}{\rho V_o} = -C^4 \tan^4 \theta \frac{p}{\pi} \left\{ \frac{1}{2} \left[\frac{(a^2+s^2)^2}{s^2} \arctan \frac{s}{a} \right]^2 + \right.$$

$$\frac{a}{s^3}(s^2-a^2)\left(a^4-6a^2s^2+s^4\right) \arctan \frac{s}{a} -$$

$$\left. \frac{\pi^2 a^4}{2} + \frac{1}{2} \frac{a^2}{s^2}(s^2-a^2)^2 \right\} \tag{19}$$

The damping-in-roll coefficient C_{l_p} based on the wing area including the part of the wing masked by the body can now be written, if both sides of the equation are multiplied by $\beta = \sqrt{|1-M_o^2|}$, in the form

$$\beta C_{l_p} = -\frac{A_r}{8\pi} \left\{ \left[(1+R^2)^2 \arctan \frac{1}{R} \right]^2 + 2R(1-R^2)(R^4-6R^2+1) \arctan \frac{1}{R} - \right.$$

$$\left. \pi^2 R^4 + R^2(1-R^2)^2 \right\} \tag{20}$$

where $R = \frac{a}{s} = \frac{A}{S}$ (i.e., the ratio of the body diameter to the wing span) and A_r is reduced aspect ratio which is also based on the total wing area including that part masked by the body.

When R equals zero, equation (20) represents the damping in roll for a wing without body. This value, which will be designated $(C_{l_p})_w$, is given by

$$\beta (C_{l_p})_w = -\frac{\pi A_r}{32} \tag{21}$$

and agrees with the value given in reference 3. The ratio of equation (20) to equation (21) represents, finally, the effect of adding a circular cylinder about the line of symmetry of any pointed, low-reduced-aspect-ratio wing with an unswept trailing edge. This effect is shown in figure 4. The figure shows that the damping in roll is increased a maximum of about 4 percent at a value of R equal to 0.28.

SWEPT-BACK WING

The study of the swept-back wing will be divided into two parts. The first of these sections will be concerned with the development of a special plan form which is relatively easy to treat analytically, while the

second section will be devoted to the examination of plan forms with arbitrary trailing edges or with arbitrary span-load distributions.

Special Plan Form

Consider a wing with a plan form similar to that shown in figure 5. The analysis of such a wing is best presented by considering separately the three regions shown in figure 5(b) which correspond, respectively, to values of x for which $x \leq 1$, $1 \leq x \leq s$, and $s \leq x$.

Region I ($x \leq 1$).- Since the loading in each region is independent of the flow at all points downstream of it, the solution for the pressures in region I is the same as that for a triangular wing. Hence region I is simply a special case of the preceding section for which the body diameter R equals zero.

Region II ($1 \leq x \leq s$).- Although each region is certainly independent of subsequent ones, the vorticity of upstream regions must be transported downstream through all subsequent transverse planes. This increases somewhat the complexity of the problem.

In order to find the solution for the loading in region II, it is again necessary to satisfy equation (1), but this time subject to the boundary conditions:

$$\left.\begin{aligned} w_o &= \mu y \quad \text{for} \quad a \leq |y| \leq b \\ u &= w = 0 \quad \text{for} \quad r = \infty, \; 0 \leq \psi < 2\pi \\ \Delta u_o &= 0 \quad \text{for} \quad 0 \leq |y| \leq a \end{aligned}\right\} \tag{22}$$

where[5] $a(x)$ and $b(x)$ are, as in the preceding section, replaced by a and b.

It is apparent that no transformation of the plane is necessary for the use of the integral equation (2), since the boundary conditions are already specified in the $z = 0$ plane. Making use of the fact that $\Delta\varphi$ must be an odd function of y, and hence its derivative Δv_o even, equation (2b) can be written

$$\frac{w_o}{y} = \mu = -\frac{1}{2\pi} \int_o^{b^2} \frac{G(x,\eta_1)\,d\eta_1}{\eta - \eta_1} \tag{23}$$

[5] Whereas in the wing-body section $a(x)$ represented the radius of the body, here $a(x)$ represents the distance from the x axis to the trailing edge. Since the two sections are entirely separate, this should cause no confusion.

where

$$\left.\begin{aligned} \eta &= y^2 \\ \text{and} \qquad G(x,\eta) &= \frac{\Delta v_o(x,y)}{y} \end{aligned}\right\} \tag{24}$$

Before the solution to equation (23) can be obtained, however, the behavior of the flow in the vortex wake, the region for which $-a \leq y \leq a$, must be discussed.

Since an increase in $\Delta\varphi_o$ corresponds to a loading $\Delta\varphi_o$ at any point behind the wing must be the same as $\Delta\varphi_o$ at the trailing edge for the same y. If the equation of the trailing edge is written in either of the forms

$$\left.\begin{aligned} y &= a(x) \\ x &= a^*(y) \end{aligned}\right\} \tag{25}$$

then $\Delta\varphi_o(x,y)$ equals $\Delta\varphi_o(a^*,y)$ for $x \geq a^*$. Taking the partial derivative of $\Delta\varphi_o(a^*,y)$ with respect to y gives

$$\frac{\partial\Delta\varphi_o(a^*,y)}{\partial y} = \frac{\partial\Delta\varphi_o(a^*,y)}{\partial a^*}\frac{da^*}{\partial y} + \left[\frac{\partial\Delta\varphi_o(x,y)}{\partial y}\right]_{x=a^*}$$

which can also be written in the form

$$\frac{\partial\Delta\varphi_o(a^*,y)}{\partial y} = \frac{V_o C}{2}\frac{da^*}{dy}\frac{\Delta p(a^*,y)}{q} + \Delta v_o(a^*,y) \tag{26}$$

Applying the Kutta condition, the value of the load coefficient at the trailing edge $\frac{\Delta p}{q}(a^*,y)$ must be zero. Equation (23) can now be written

$$\mu = -\frac{1}{2\pi}\int_o^{a^2}\frac{G^*(\eta_1)d\eta_1}{\eta-\eta_1} - \frac{1}{2\pi}\int_{a^2}^{b^2}\frac{G(x,\eta_1)d\eta_1}{\eta-\eta_1} \tag{27}$$

where $G^*(\eta_1) = G(a^*,\eta_1)$.

The value of $G^*(\eta_1)$ depends, of course, on the equation of the trailing edge. It is convenient at this stage of the analysis to choose the value of $\Delta\varphi_o$ in the wake (since applying the Kutta condition to equation (26) yields $G^*(\eta_1) = \frac{1}{y}\left[\frac{\partial\Delta\varphi_o(x,y)}{\partial y}\right]_{x=a^*}$, giving $\Delta\varphi_o$ is equivalent

to specifying $G^*(\eta_1)$) and find the resulting trailing edge rather than to proceed in the more straightforward way of first completely specifying the wing plan form. However, if $\Delta\varphi_o$ is expressed in the form

$$\frac{\Delta\varphi_o}{-\mu} = B_1 y + B_2 y^2 + \ldots + B_m y^m \tag{28a}$$

it will be shown that both the trailing edge and the final value of $C\dot{l}_p$ can be given in terms of the B_n's, and, therefore, quite general types of plan forms can be analyzed. Our purpose is to present in some detail the simplest example in this section and to develop the general discussion later.

Figure 6 shows the variation of $\Delta\varphi_o$ in the wake behind a triangular wing (equation (15) with $a = 0$, $b = 1$). A reasonable first choice of $\Delta\varphi_o$ in the wake of a swept-back wing would seem to be the straight-line continuation of the slope at the origin of figure 6. This leads to the equations

$$B_1 = 1, \quad B_2 = B_3 = \ldots = 0$$

so that equation (28a) becomes

$$G^*(\eta_1) = -\mu/\sqrt{\eta_1} \tag{28b}$$

If $G(x,\eta_1)$ is defined by the relation[6]

$$G(x,\eta_1) = G_1(x,\eta_1) + H(x)\sqrt{\frac{\eta_1 - a^2}{b^2 - \eta_1}} \tag{29}$$

where $H(x)$ is a function to be determined independent of η_1, then equation (27) can be written

$$\mu - \frac{\mu}{2\pi}\int_0^{a^2} \frac{d\eta_1}{(\eta - \eta_1)\sqrt{\eta_1}} - \frac{H(x)}{2} = -\frac{1}{2\pi}\int_{a^2}^{b^2} \frac{G_1(x,\eta_1)\,d\eta_1}{\eta - \eta_1} \tag{30}$$

It is now possible to invert equation (30) by means of equation (12), wherein a^2 now replaces $-b_1$ and b^2 replaces b_1. First we notice that the condition imposed by equation (11) is satisfied if

---

[6]The choice of such a definition is, of course, not obvious. Its advisability depends entirely on the simplification which it introduces into the subsequent analysis.

$$\int_{a^2}^{b^2} \left[\mu - \frac{\mu}{2\pi} \int_{o}^{a^2} \frac{d\eta_1}{(\eta-\eta_1)\sqrt{\eta_1}} - \frac{H(x)}{2} \right] \frac{d\eta}{\sqrt{(b^2-\eta)(\eta-a^2)}} = 0$$

or, upon integrating, that

$$H(x) = \frac{2\mu}{\pi} \left(\pi - \frac{K}{b} \right)$$

where K is the complete elliptic integral of the first kind of modulus $k = \frac{a}{b}$. The solution for $G_1(x,\eta)$ in the interval $a \leq |y| \leq b$ becomes

$$G_1(x,\eta) = \frac{2}{\pi} \sqrt{(b^2-\eta)(\eta-a^2)} \int_{a^2}^{b^2} \frac{\left[\frac{\mu K}{\pi b} - \frac{\mu}{2\pi} \int_{o}^{a^2} \frac{d\eta_2}{(\eta_1-\eta_2)\sqrt{\eta_2}} \right] d\eta_1}{(\eta-\eta_1)\sqrt{(b^2-\eta_1)(\eta_1-a^2)}}$$

The single integral evaluates to give zero, and the order of the double integral can be reversed and integrated with respect to η_1 so that finally there results

$$G_1(x,\eta) = -\frac{\mu}{\pi} \sqrt{(b^2-\eta)(\eta-a^2)} \int_{o}^{a^2} \frac{d\eta_2}{(\eta-\eta_2)\sqrt{\eta_2(b^2-\eta_2)(a^2-\eta_2)}}$$

Using equation (29), we can now write

$$G(x,\eta) = \frac{-\mu}{\pi} \int_{o}^{a^2} \frac{d\eta_2 \sqrt{(b^2-\eta)(\eta-a^2)}}{(\eta-\eta_2)\sqrt{\eta_1(b^2-\eta_2)(a^2-\eta_2)}} + \frac{2\mu}{\pi} \left(\pi - \frac{K}{b} \right) \sqrt{\frac{\eta-a^2}{b^2-\eta}} \tag{31}$$

Now using the equality

$$(\Delta\varphi)_{T.E.} = \Gamma = \frac{1}{2} \int_{b^2}^{a^2} G(x,\eta) d\eta$$

it is possible to derive, after some manipulation, the relation

$$\Gamma = -\mu b \left(\frac{1}{2} k'^2 K - E + k \right) - \left(\pi - \frac{K}{b} \right) \frac{\mu}{2} b^2 k'^2 \tag{32}$$

where K and E are complete elliptical integrals of the first and second kind, respectively, of modulus $k = \sqrt{1 - k'^2} = \frac{a}{b}$.

For the Kutta condition to apply at the trailing edge, equation (32) must reduce to the expression $\Gamma = -y_{T.E.}\ \mu = -a\mu$ in the interval $-t \leq y \leq t$ (region II, fig. 5). This leads to the equation for the trailing edge in region II given by

$$a = \frac{2kE}{\pi k'^2} \tag{33}$$

Figure 7 shows a plot of the trailing edge derived from equation (33). The asymptotic slope of this edge is 45° and the asymptotic width of the wing (i.e., $b-a$ as $b \rightarrow \infty$) can be shown to be $1/\pi$. By means of this plot, it is possible to find the relation between aspect ratio and semispan s, for wings of the type shown in figure 5. This was done numerically and the results are shown for two different tip conditions in figure 8.

Region III ($x \geq s$).- Consider for a moment that the wing plan form ends with region II; that is, the wing has the form designated as type b in figure 8. The downwash in any plane behind the straight portion of the trailing edge of such a wing is determined by substituting equations (31) and (28b) into equation (23) and integrating. Designating this value of w_o as w_∞, there results for $t \leq |y| \leq s$

$$w_\infty = y\mu$$

and for $0 \leq |y| \leq t$

$$w_\infty = y\mu \left[1 + \left(\frac{K_1}{\pi t} - 1\right)\sqrt{\frac{t^2-y^2}{s^2-y^2}}\right] - \frac{p}{\pi}\left[K_1 E_1\left(\frac{y}{t}\right) - E_1 F_1\left(\frac{y}{t}\right)\right] \tag{34}$$

where $E_1\left(\frac{y}{t}\right)$ and $F_1\left(\frac{y}{t}\right)$ are the incomplete elliptic integrals with modulus $k_1 = t/s$ and argument y/t, and K_1 is the complete form of $F_1\left(\frac{y}{t}\right)$. It should be noticed that behind the straight portion the flow is turning as if the wing were continued. Hence, any surface behind the straight part of the trailing edges of the type b wing will support zero loading, provided, of course, this surface is also rotating at the rate $w = \mu y$. Thus the solution for the type a wing is exactly the same as that for the type b wing with the added condition that the loading is zero over portions of the wing for which $x > s$.

Results for entire wing.- The results for the entire wing plan form can be summarized in the form of the total rolling moment and

subsequently the value of C_{l_p}. The rolling moment for both types of wings is found from the expression

$$L = 2\rho V_o C^2 \tan^2 \theta \int_o^s y\Gamma dy \tag{35}$$

Using the solution for Γ given by operating on equation (31), that is for $0 \leq |y| \leq t$

$$\Gamma = -\mu y$$

and for $t \leq |y| \leq s$

$$\Gamma = -\frac{\mu}{2\pi} \int_{s^2}^{y^2} d\eta \int_o^{t^2} \frac{d\eta_1}{\eta - \eta_1} \sqrt{\frac{(s^2-\eta)(\eta-t^2)}{\eta_1(s^2-\eta_1)(t^2-\eta_1)}} + \frac{\mu}{2} \int_{s^2}^{y^2} \sqrt{\frac{\eta-t^2}{s^2-\eta}}\, d\eta$$

in equation (35) and reversing the order of integration, the value of the moment can be obtained in coefficient form as

$$\frac{\beta C_{l_p}}{\beta \tan \theta} = -\frac{1}{4} \frac{A_r}{\beta \tan \theta} \left(\frac{3}{8} \pi k_1'^4 + \frac{5k_1^2 - 1}{6s} E_1 - \frac{1}{3} k_1'^2 \frac{K_1}{s} \right) \tag{36}$$

where again β has been introduced as a multiplier of spanwise and vertical lengths and where $k_1 = t/s = \sqrt{1 - k_1'^2}$. Equation (36) is plotted in figure 9 for the plan-form-aspect-ratio relation given in figure 8. When k_1 is zero, equation (36) reduces to equation (21) for the triangular wing.

Arbitrary Plan Form

If all the terms in equation (28a) are considered then equation (28b) becomes

$$G^*(\eta_1) = -\mu \sum_{n=1}^{m} n B_n \eta_1^{\frac{n-2}{2}} \tag{28c}$$

and, using equation (29), equation (30) can be written

$$\mu + \sum_{n=1}^{m} \frac{-\mu n B_n}{2\pi} \int_0^{a^2} \frac{\eta_1^{\frac{n-2}{2}} d\eta_1}{\eta-\eta_1} - \frac{H(x)}{2} = -\frac{1}{2\pi} \int_{a^2}^{b^2} \frac{G_1(x,\eta_1)d\eta_1}{\eta-\eta_1} \tag{37}$$

Now if

$$H(x) = 2\mu - \frac{2\mu}{\pi b} \sum_{n=1}^{m} n B_n a^{n-1} \int_0^K sn^{n-1} u \, du$$

then

$$G_1(x,\eta) = \frac{2}{\pi}\sqrt{(b^2-\eta)(\eta-a^2)} \int_{a^2}^{b^2} \frac{d\eta_2}{(\eta-\eta_2)\sqrt{(b^2-\eta_2)(\eta_2-a^2)}} \sum_{n=1}^{m} \frac{-\mu n B_n}{2\pi} \int_0^{a^2} \frac{\eta_1^{\frac{n-2}{2}} d\eta_1}{\eta-\eta_1} \tag{38}$$

and, finally,

$$\Gamma = \frac{\mu b}{2} \sum_{n=1}^{m} n B_n a^{n-1} \int_0^K \left[(1+k^2) sn^{n-1} u - 2k^2 sn^{n+1} u \right] du - \mu \sum_{n=1}^{m} B_n a^n -$$

$$2\mu \frac{\pi}{4} b^2 k'^2 + \frac{b k'^2 \mu}{2} \sum_{n=1}^{m} n B_n a^{n-1} \int_0^K sn^{n-1} u \, du \tag{39}$$

In order to satisfy the Kutta condition, Γ in equation (39) must equal $-\mu \sum_{n=1}^{m} B_n a^n$. Thus, the equation of the trailing edge becomes

$$a = \frac{2k}{\pi k'^2} \sum_{n=1}^{m} n B_n a^{n-1} I_n \tag{40}$$

and, using equation (35), the expression for rolling-moment coefficient becomes

$$\frac{\beta C_{l_p}}{\beta \tan\theta} = \frac{A_r}{4s\beta \tan\theta} \sum_{n=1}^{m} n B_n k_1^{n-1} s^{n-1} \left(k_1^2 I_{n+2} + \frac{1-3k_1^2}{2} I_n \right) - \frac{3\pi k_1'^4}{32} \tag{41}$$

where

$$I_n = \int_0^K \left(sn^{n-1}u - k^2 sn^{n+1}u \right) du = \int_0^1 \tau^{n-1} \sqrt{\frac{1-k_1^2\tau^2}{1-\tau^2}}\, d\tau \qquad (42)$$

Values of the first six I_n are given in Appendix B.

Since the trailing edge must pass through the point $a = 0$ when $x = 1$, the value of B_1 must always be 1. The other coefficients, however, are at our disposal. These can be determined by specifying the points through which the trailing edge must pass and setting up a series of simultaneous equations using equation (40).

Two examples have been considered which represent a wing with very little taper (fig. 10(a)) and a wing which tapers to a point (fig. 10(b)). The trailing edge for the former of these wings, type c, was found by finding the values of B_2 in equation (40) which made $a = 0.4$ when $b = 1.2$ and all the B's with higher subscripts were zero. The trailing edge of the latter of the two wings, type d, was determined by finding B_2, B_3, B_4, and B_5 such that the edge passed through four points which were on a straight line joining the root with the tip. Figure 11 shows the actual edge resulting for the type d wing together with the intended straight line and the points chosen. The slight scallop indicated in the trailing edge was found in the case of the triangular wing (i.e., when this method was used to solve the delta-shaped wing and the results compared with the exact solution of the linearized equation) to give a value of $\frac{\beta C_{l_p}}{\beta \tan \theta}$ about 5 percent too low. However, this was considered to be sufficiently accurate to establish the trend which is shown for this type of wing in figure 12.

Ames Aeronautical Laboratory,
National Advisory Committee for Aeronautics,
Moffett Field, Calif., July 22, 1949.

APPENDIX A

TABLE OF IMPORTANT SYMBOLS

a, a(x)	radius of cylindrical body in transformed space (in portion of report titled "Triangular Wing with Body")
a, a(x), a*(y)	equation of trailing edge of swept wing in transformed space (in portion of report titled "Swept-Back Wing," see equation (25))

$A(X)$	radius of cylindrical body or equation of trailing edge
A_r	reduced aspect ratio, $\sqrt{\lvert 1-M_o^2 \rvert}$ times aspect ratio
b, $b(x)$	equation of wing leading edge in transformed space
$B(X)$	equation of wing leading edge
C	root chord of wing
C_l	$\dfrac{\text{rolling moment}}{(2qS)(\text{wing area})}$
C_{l_p}	damping-in-roll coefficient $\left[\dfrac{\partial C_l}{\partial(pS/V_o)} \right]$
$\left(C_{l_p} \right)_w$	damping-in-roll coefficient of wing alone
E_1	complete elliptic integral of the second kind with modulus k_1
$E_1(x)$	incomplete elliptic integral $\left(\int_o^x \sqrt{\dfrac{1-k_1^2t^2}{1-t^2}}\, dt \right)$
$G(x,\eta)$	function introduced in equation (24)
K_1	complete elliptic integral of the first kind with modulus k_1
$F_1(x)$	incomplete elliptic integral $\left[\int_o^x \dfrac{dt}{\sqrt{(1-k_1^2t^2)(1-t^2)}} \right]$
k	$\dfrac{a}{b}$
k_1	$\dfrac{t}{s}$
l	lift
L	rolling moment
M_o	Mach number of free stream

p	rate of roll, radians per second
q	dynamic pressure $\left(\frac{1}{2}\rho V_o^2\right)$
r	radial length in polar coordinates
R	ratio of body diameter to wing span
s	wing semispan in transformed space
S	wing semispan
$sn(u)$	Jacobian elliptic function
T,t	distance used in study of swept-back wing (see fig. 5)
V_o	free-stream velocity
u, v, w	transformed perturbation-velocity components in x,y,z directions, respectively
v_r	radial component of velocity
u_t, v_t, w_t	perturbation-velocity components in X,Y,Z directions, respectively
x, y, z	transformed Cartesian coordinates
X, Y, Z	Cartesian coordinates in physical plane
β	$\sqrt{\lvert 1 - M_o^2 \rvert}$
$\frac{\Delta p}{q}$	loading coefficient, $\left(\frac{\text{pressure on lower surface} - \text{pressure on upper surface}}{q}\right)$
Γ	spanwise distribution of circulation
η	y^2
θ	semiapex angle of wing
μ	$pC^2 \tan^2 \theta$
ξ	complex variable $(y + iz)$
ρ	free-stream density
Φ	perturbation potential

φ perturbation potential in transformed coordinates

$\Delta\varphi_o$ jump in potential in the $z = 0$ plane

ψ polar angle

APPENDIX B

Exact expressions for $I_1, I_2, \ldots I_6$.

$$I_1 = E$$

$$I_2 = \frac{1}{2} + \frac{k'^2}{4k} \ln \frac{1+k}{1-k}$$

$$I_3 = \frac{1}{3k^2} \left[k'^2 K - (1-2k^2) E \right]$$

$$I_4 = \frac{1}{4} - \frac{1}{8} \frac{k'^2}{k^2} \left(1 - \frac{1+3k^2}{2k} \ln \frac{1+k}{1-k} \right)$$

$$I_5 = \left[\frac{3}{5} + \frac{2(1-4k^2)(1+k^2)}{15k^2} \right] \frac{K-E}{k^2} - \frac{1-4k^2}{15k^2} K$$

$$I_6 = - \frac{(1+3k^2)(3-5k^2)}{48k^4} + \frac{(1-k^2)(1+2k^2+5k^4)}{32k^5} \ln \frac{1+k}{1-k}$$

Notice that when $k=1$, $I_n = \frac{1}{n}$.

Series expansions for $I_1, I_2, \ldots I_6$ for $k<1$.

$$I_1 = \frac{\pi}{2} \left(1 - \frac{k^2}{4} - \frac{3}{64} k^4 - \frac{5}{256} k^6 - \ldots \right)$$

$$I_2 = 1 - \frac{1}{3} k^2 - \frac{1}{15} k^4 - \frac{1}{35} k^6 - \ldots$$

$$I_3 = \frac{\pi}{4} \left(1 - \frac{3}{8} k^2 - \frac{5}{64} k^4 - \frac{35}{1024} k^6 - \ldots \right)$$

$$I_4 = \frac{2}{3} - \frac{4}{15} k^2 - \frac{2}{35} k^4 - \frac{8}{315} k^6 - \ldots$$

$$I_5 = \frac{\pi}{16} \left(3 - \frac{5}{4} k^2 - \frac{35}{128} k^4 - \frac{63}{512} k^6 - \ldots \right)$$

$$I_6 = \frac{8}{15} - \frac{8}{35} k^2 - \frac{16}{315} k^4 - \frac{16}{693} k^6 - \ldots$$

REFERENCES

1. Jones, R. T.: Properties of Low-Aspect-Ratio Pointed Wings at Speeds Below and Above the Speed of Sound. NACA Rep. 835, 1946.

2. Heaslet, Max. A., Lomax, Harvard, and Spreiter, John R.: Linearized Compressible-Flow Theory for Sonic Flight Speeds. NACA TN 1824, 1949.

3. Ribner, Herbert S.: The Stability Derivatives of Low-Aspect-Ratio Triangular Wings at Subsonic and Supersonic Speeds. NACA TN 1423, 1947.

4. Spreiter, John R.: Aerodynamic Properties of Slender Wing-Body Combinations at Subsonic, Transonic, and Supersonic Speeds. NACA TN 1662, 1948.

5. Spreiter, John R.: Aerodynamic Properties of Cruciform-Wing and Body Combinations at Subsonic, Transonic, and Supersonic Speeds. NACA TN 1897, 1949.

6. Heaslet, Max. A., and Lomax, Harvard: The Application of Green's Theorem to the Solution of Boundary-Value Problems in Linearized Supersonic Wing Theory. NACA TN 1767, 1949.

7. Brown, Clinton E., and Adams, Mac C.: Damping in Pitch and Roll of Triangular Wings at Supersonic Speeds. NACA TN 1566, 1948.

8. Allen, H. Julian: General Theory of Airfoil Sections Having Arbitrary Shape or Pressure Distribution, NACA Rep. 833, 1945.

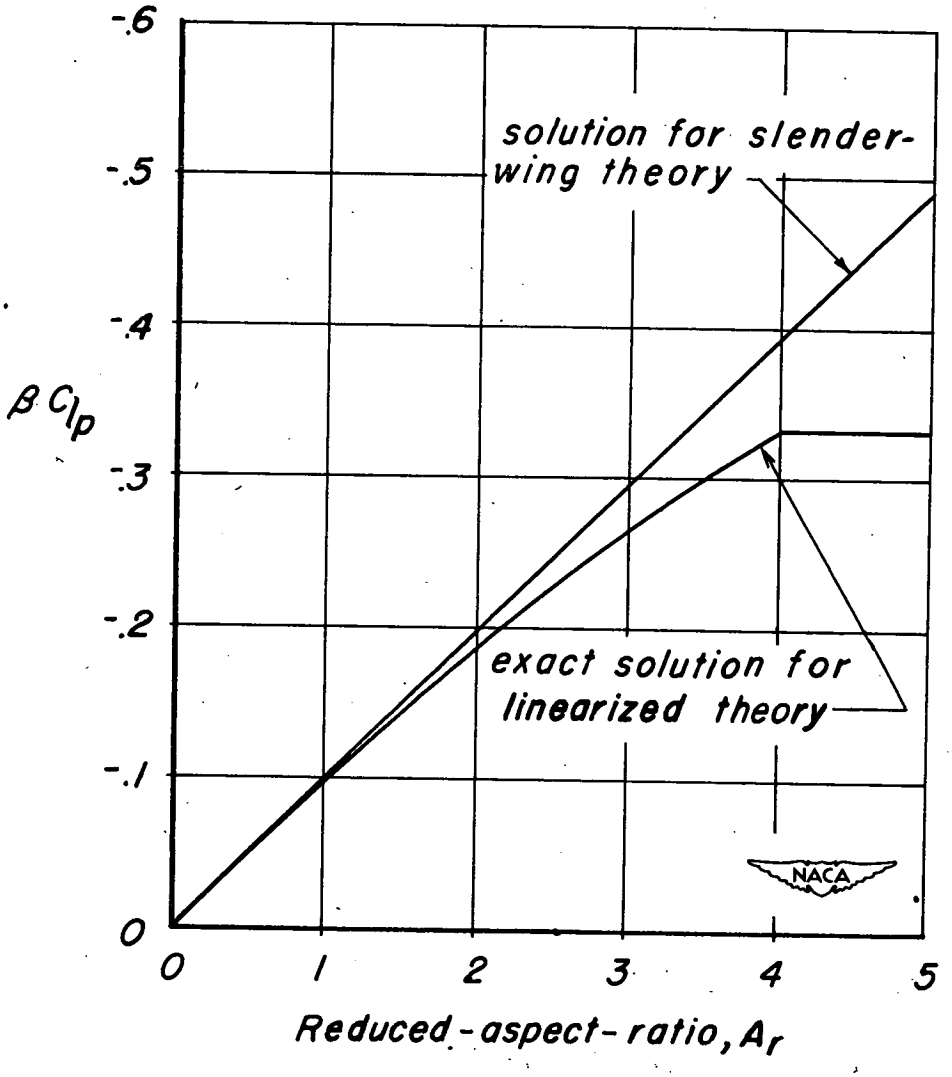

Figure 1.- Comparison of two theoretical results for a rolling triangular wing.

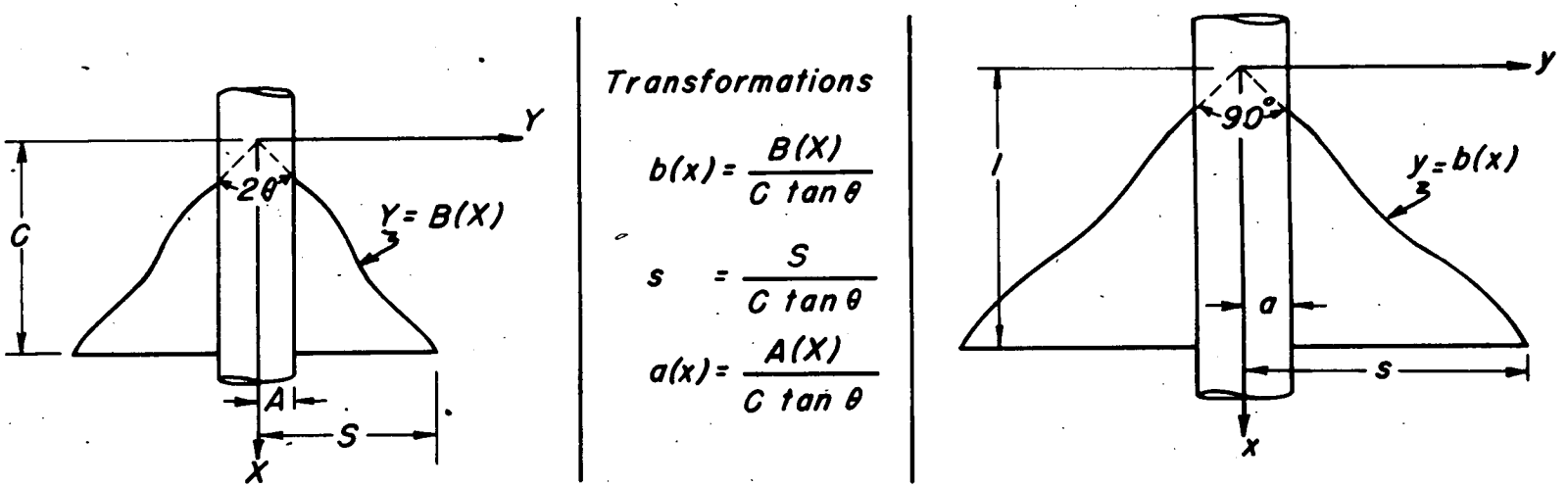

(a) True space.

(b) Transformed space.

Figure 2.- Dimensions and transformations used in analysis of rolling wing with body.

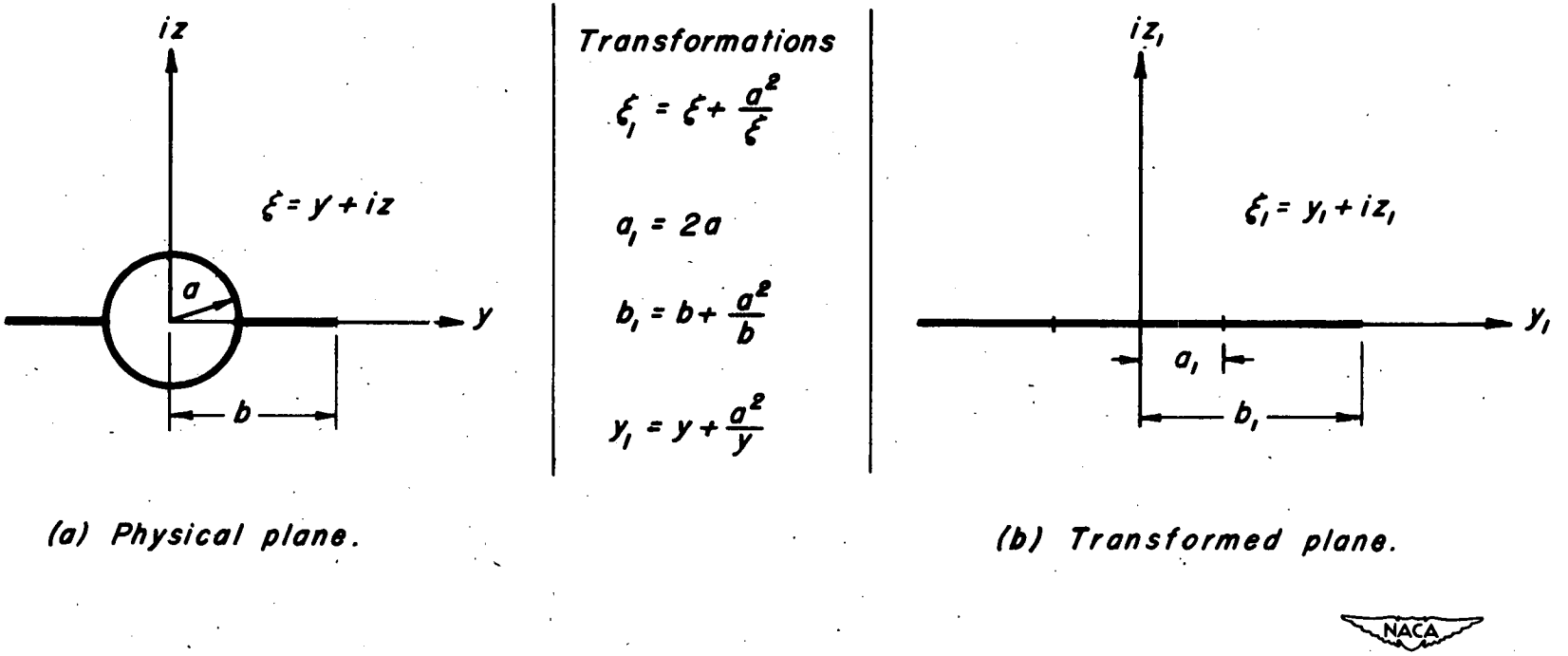

Figure 3.- Physical and transformed planes used in analysis of rolling wing with body.

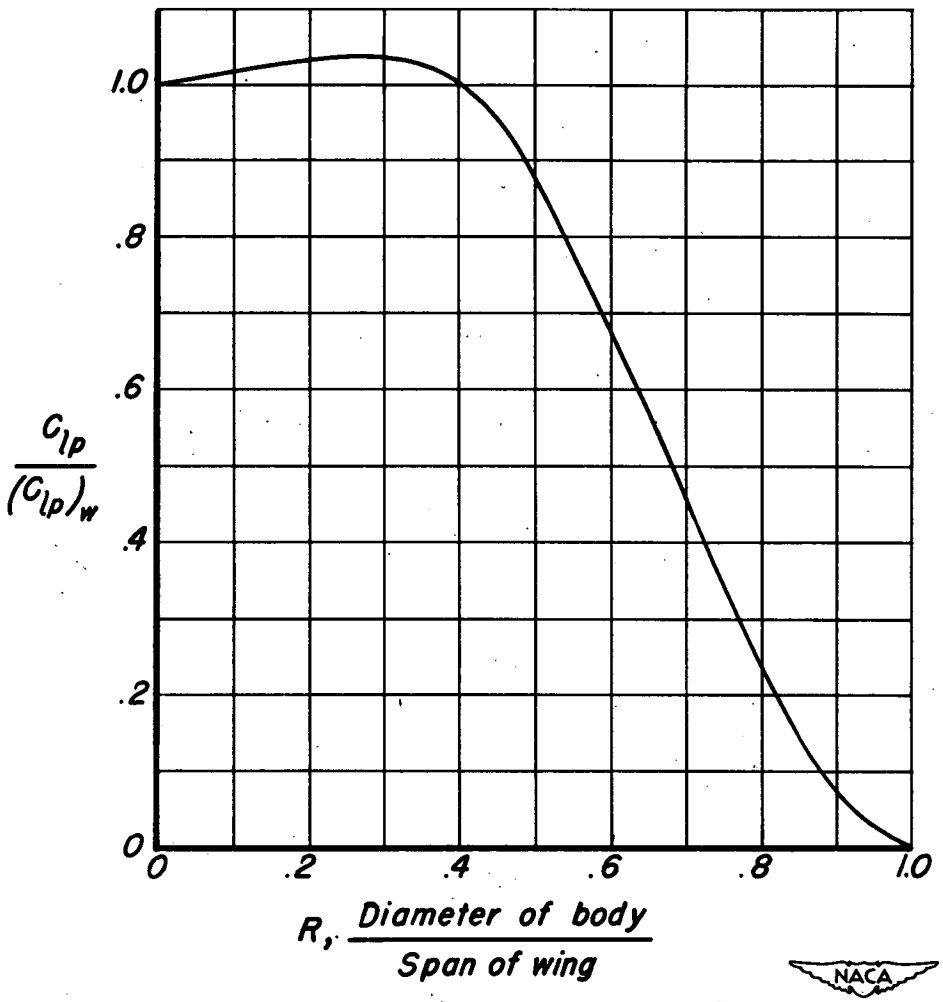

Figure 4.- Effect on damping in roll of a cylindrical body mounted on a pointed wing with unswept trailing edge.

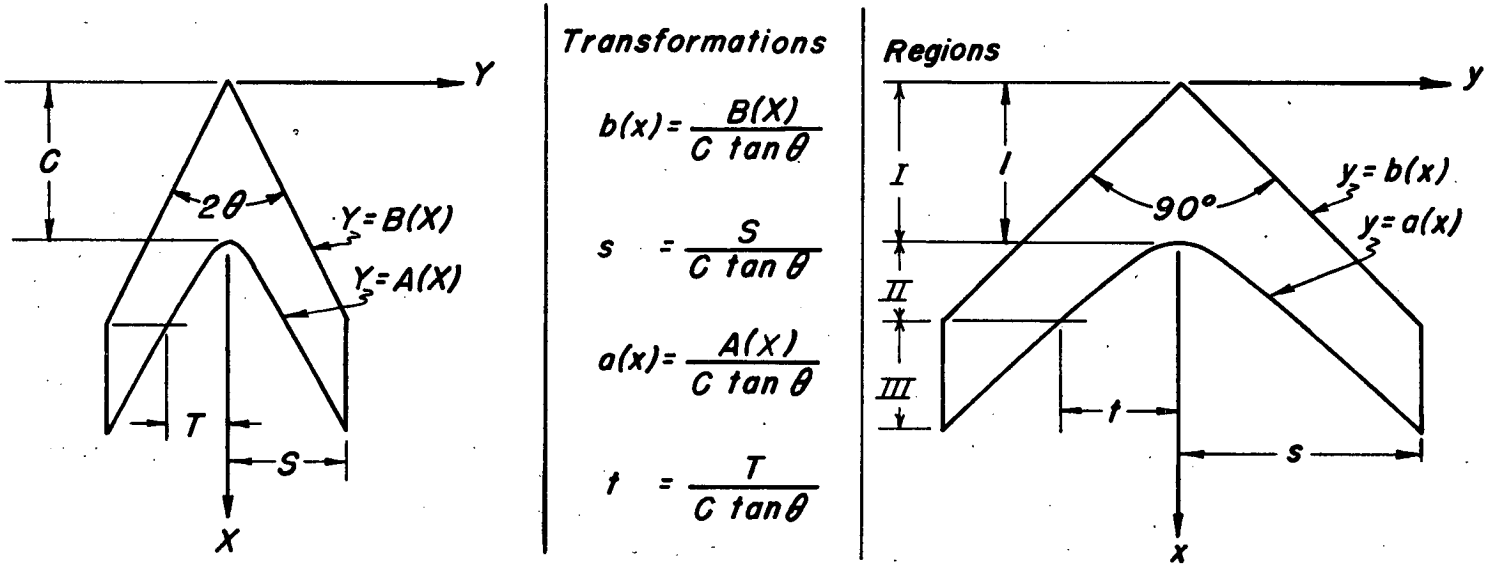

(a) True space.

(b) Transformed space.

Figure 5.- Dimensions, transformations, and regions used in analysis of rolling swept-back wing.

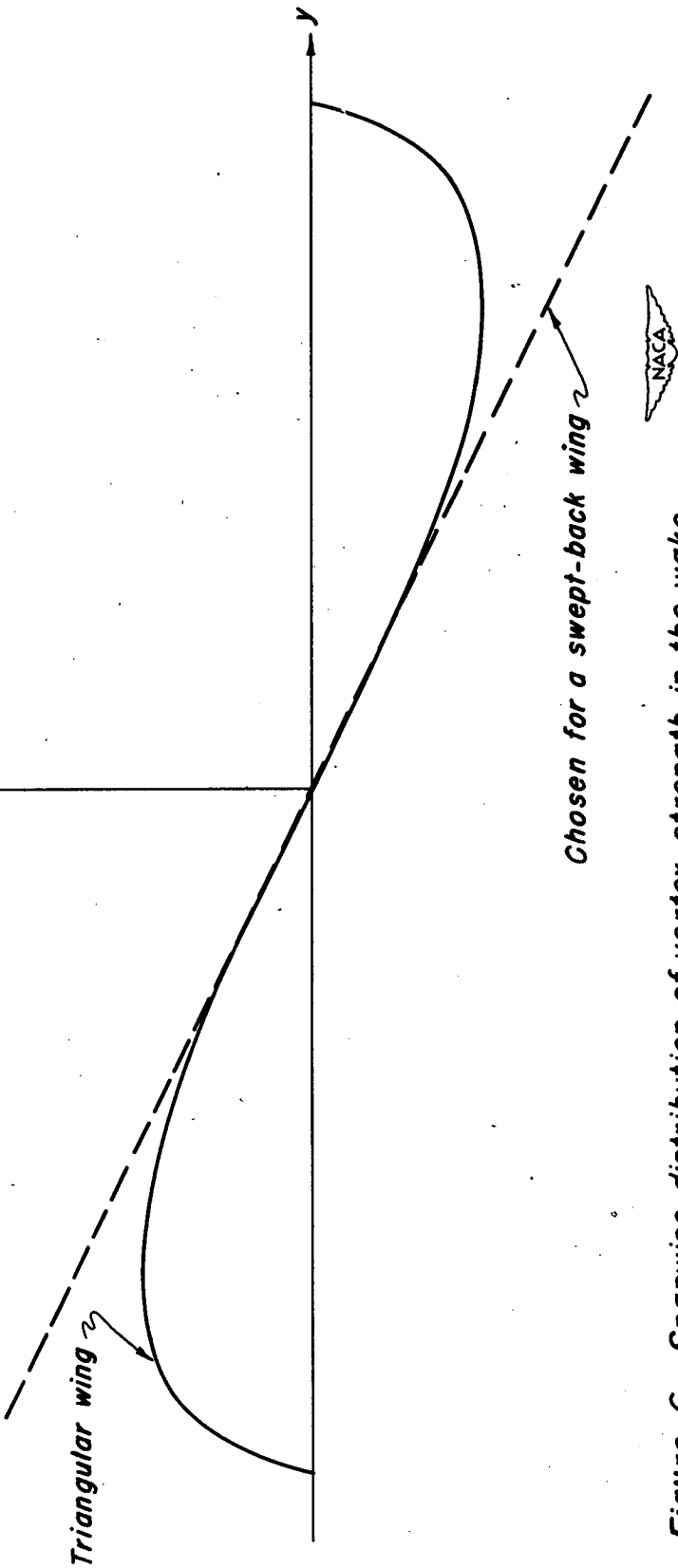

Figure 6.- Spanwise distribution of vortex strength in the wake.

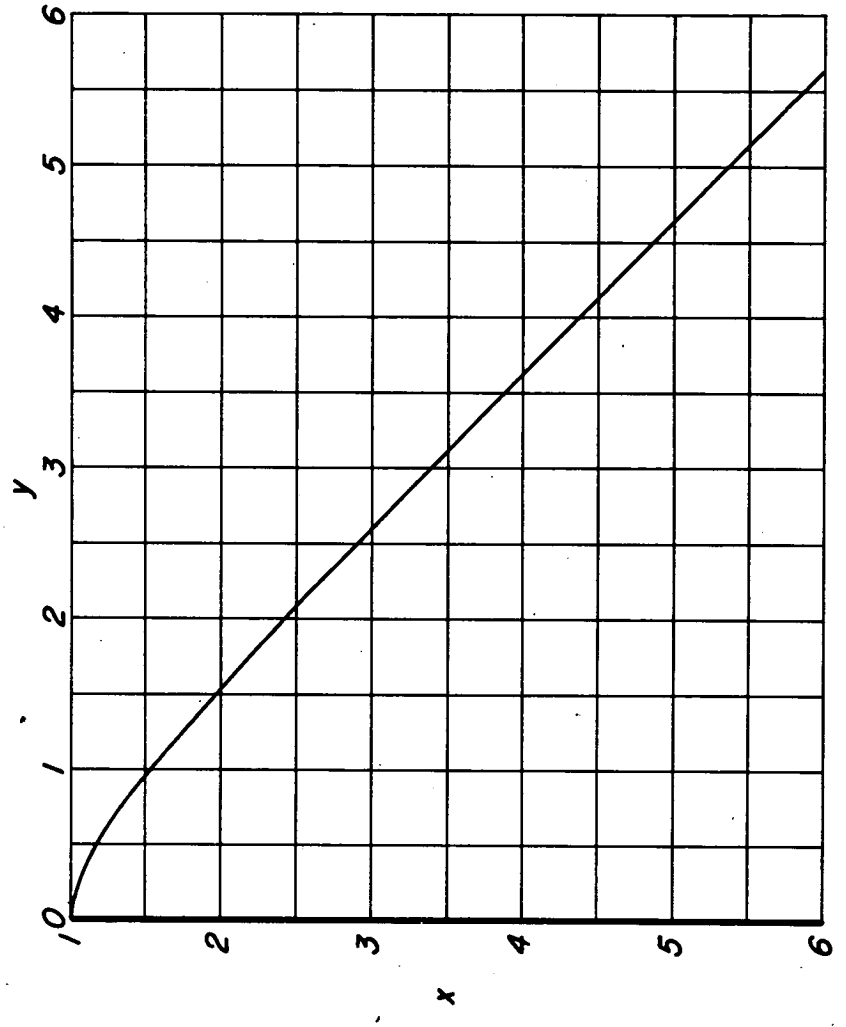

Figure 7.- Graph of trailing edge $y = a(x)$ for special swept-back wing.

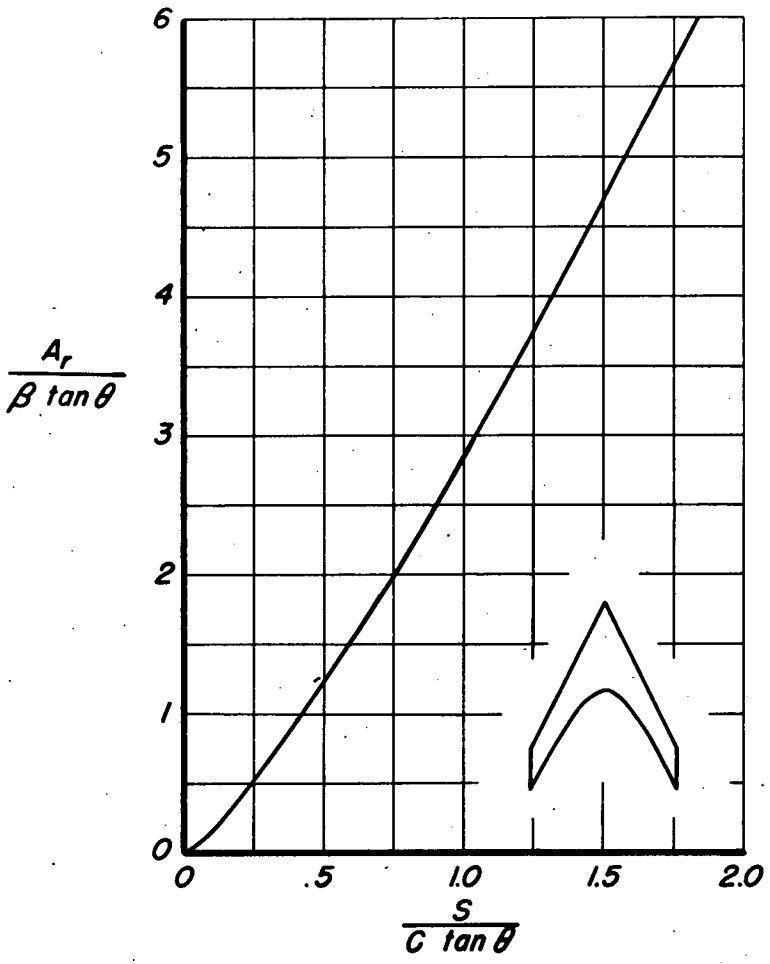

(a) Type a.

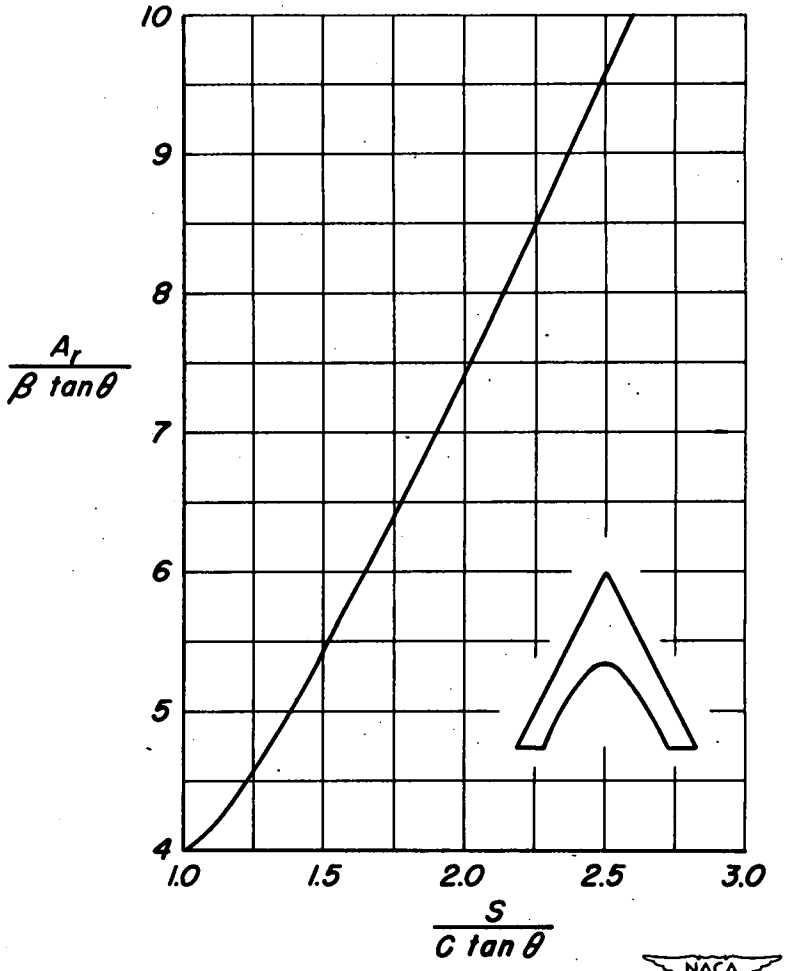

(b) Type b.

Figure 8.- Relation between aspect ratio and wing semispan for two types of swept-back wings.

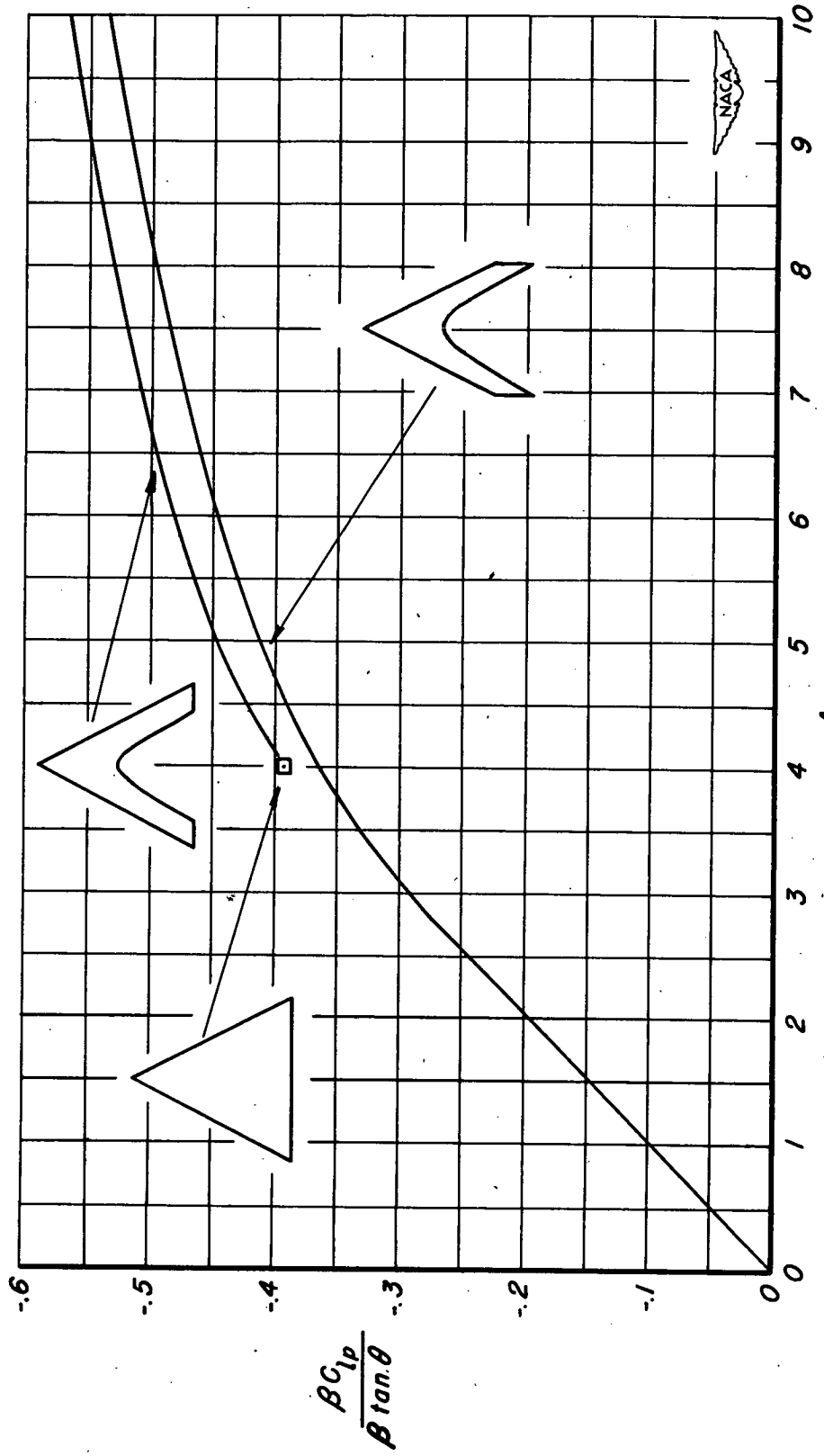

Figure 9.- Variation of damping-in-roll parameter with reduced-aspect-ratio parameter for low values of reduced aspect ratio.

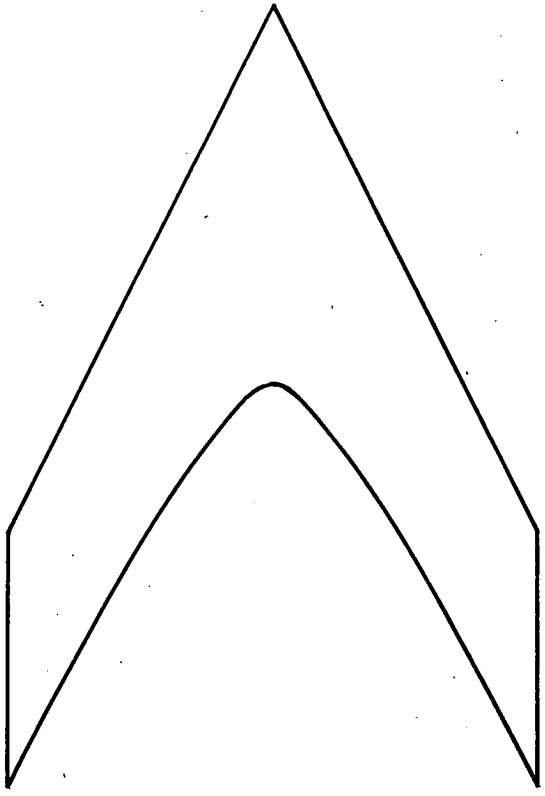

(a) Type c.

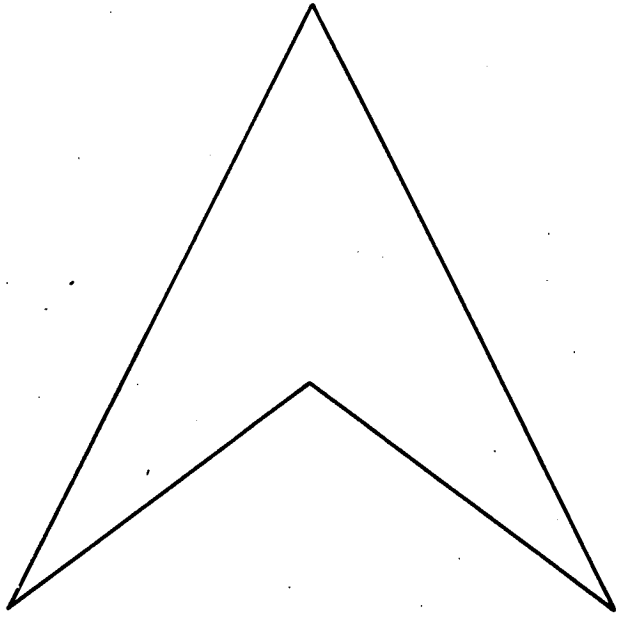

(b) Type d.

Figure 10.- Two swept-back wing plan forms studied.

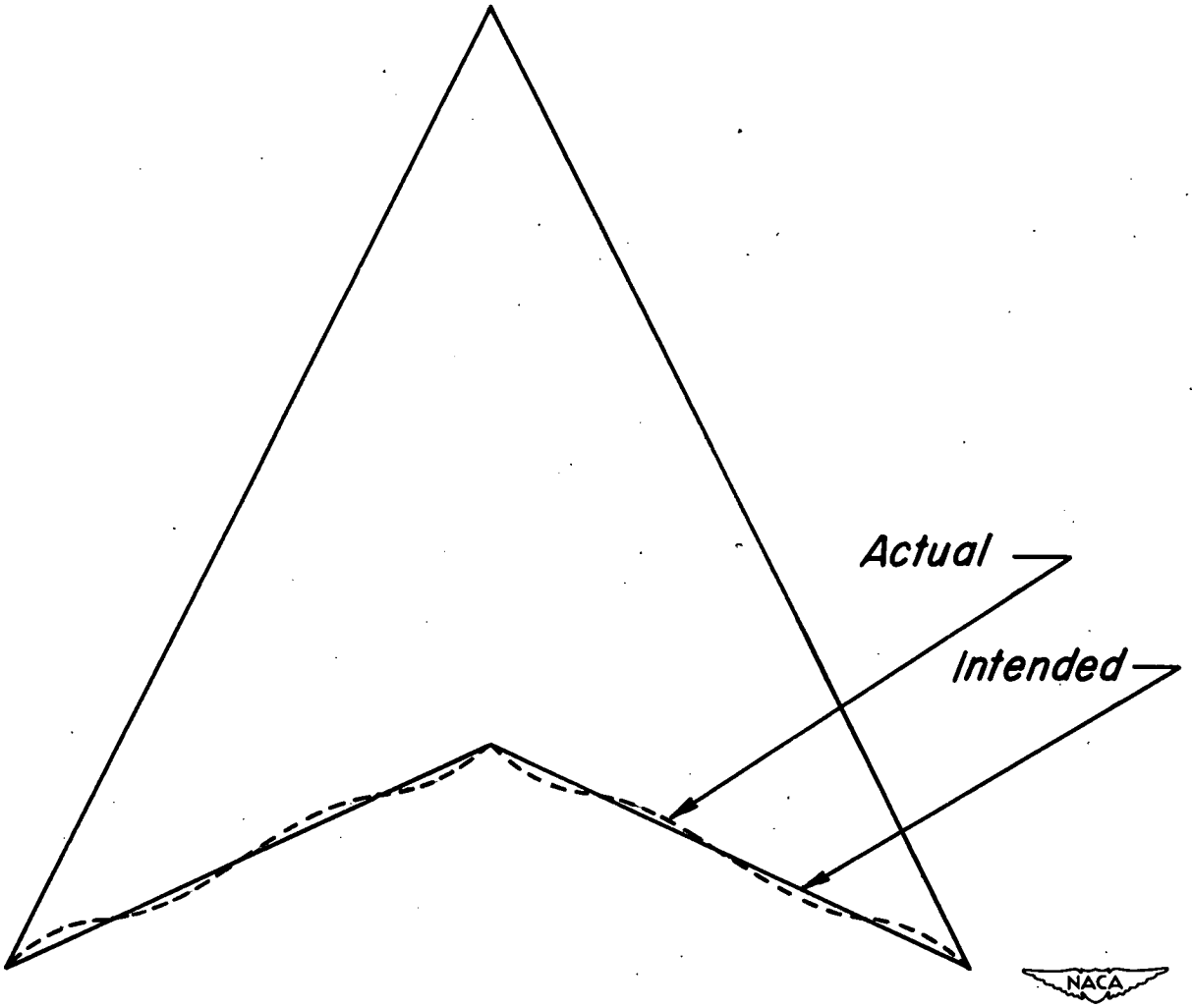

Figure 11. – Comparison of actual with intended trailing edge.

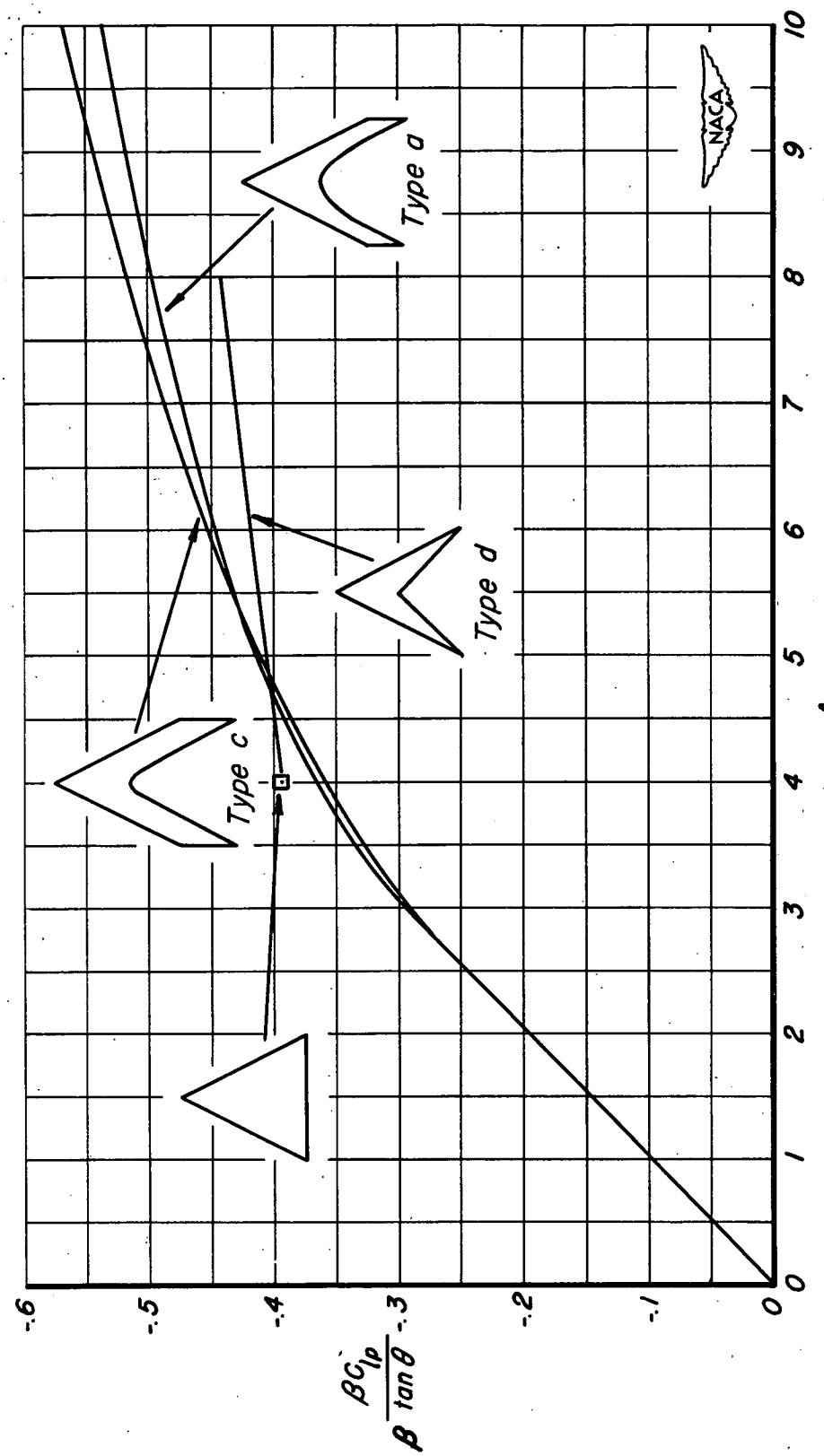

Figure 12.- Variation of damping-in-roll parameter with reduced-aspect-ratio parameter for various wing plan forms and for low values of reduced aspect ratio.

NACA-Langley - 9-21-49 - 1,000